

26 performed, followed by recommendations to avoid these failures in the future. Moreover,
27 a computational fluid dynamics (CFD) simulation was performed in order to help in the
28 failure determination and the key recommendations to avoid the most common and
29 frequent failures.

30 **Keywords:** pipeline, waste management, pneumatic waste collection, failure analysis,
31 Automated Waste Collection System (AWCS), waste management, Computational Fluid
32 Dynamics (CFD)

33 **1. Introduction**

34 Traditional systems of municipal waste management rely on the waste collection and
35 storage in dumpsters until their recollection and transport by a local waste management
36 agency. Although these systems are really flexible, they have important drawbacks and
37 environmental impacts, such as odours and plagues due to the waste accumulation in the
38 dumpsters, hygiene problems, noise, traffic congestions and greenhouse emissions from
39 garbage trucks used to waste transport, among others (Hedden, 1975).

40 Therefore, in the last years the installation of a pneumatic underground collection system,
41 like Automated Waste Collection System (AWCS) and Automated Vacuum Waste
42 Collection (AVWC) systems, has increased due its high collection efficiency and eco-
43 friendly waste management. AWCS and AVWC systems are based on the garbage
44 collection and transport via underground pneumatic pipelines to the treatment plants,
45 hence they eliminate the environmental impact and drawbacks of the traditional systems.
46 This is reported in comparative studies of the overall potential impact of different
47 collection systems, like AWCS, multi-container and door-to-door, using Life Cycle
48 Assessment (LCA) or Life Cycle Inventor. The implementation of a pneumatic waste
49 collection system produces a local reduction of the CO₂ emissions, a less traffic
50 congestion and a decrease of the energy demand due to the transport of the garbage via

51 underground than by trucks (Chàfer et al., 2019; Iriarte et al., 2009; Kogler, 2007;
52 Punkkinen et al., 2012). Moreover, in the J. H. Oh et al. study is reported that the city
53 with an AVCS presents lower general waste generation per capita than the city with
54 conventional garbage trucks (Oh et al., 2016).

55 Although these systems require significant capital costs to implement, they have
56 improved environmental characteristics and lower operating costs than conventional
57 systems. As it is reported in the study of Nakou et al. in where makes a financial and
58 economic evaluation of use AVCS in Athens, Greece (Nakou et al., 2014).

59 Teerioja et al. make a hypothetical economic comparison between AWCS and door-to-
60 door system in an existing and dense populated area, Helsinki, Finland (Teerioja et al.,
61 2012). It is concluded that the door-to-door system is six times more economic that
62 AWCS, due to the high cost to install the AWCS in an already constructed residential
63 area and suggesting that in new residential areas the cost will be reduced. Nevertheless,
64 the key factor is the large investment cost and the economic value of the land.

65 The pneumatic collection system is not a novel idea (Zandi and Hayden, 1969). The firsts
66 AWCS and AVWC factories appeared in the 70s, as in the commercial complex Disney
67 World, Florida, USA (1971), the Summint Plaza, Jersey, USA (1972), Roosevelt Island,
68 USA (1975), Barcelona Spain (1992), Leon Spain (1997) and hospitals (Bravo, 1975;
69 Dallaire, 1974; Jackson, 2004; Kown, B. T; Kass, 1973; Laux-bachand, 2003).
70 Nowadays, the studies of the pneumatic waste collection systems reside on factories
71 optimization using new mobilization techniques (Esar Fern Andez A et al., 2015;
72 Fernández et al., 2014) and in their implementation on the smart cities infrastructures
73 (Popa et al., 2017).

74 Designing and constructing AWCS remains a technology challenge. To fully understand
75 the magnitude of this challenge, one must take into account the extreme conditions that
76 affect the various components of AWCS systems. One of the most critical components of
77 these systems that is directly linked to the viability of the AWCS factory are the pipes.
78 The pipes are in direct contact with the waste transported at high velocities, where the
79 waste may have all types of geometries and dimensions, and may contain improper
80 components of the recollected fraction, like glass and other ceramic material of high
81 hardness; this entails the attrition of pipes. Wear due to abrasion and erosion has a severe
82 adverse effect on pipelines, joints and elbows. (Njobuenwu and Fairweather, 2012;
83 Zdravecká et al., 2014). At the same time, the pipes are subjected not only to possible
84 corrosive conditions on the ground where they are installed, also to the acidity produced
85 by the organic waste they can transport (Reyes, 2015).

86 In order to move forward in the construction and design of AWCS factories, and in
87 particular in its pipes, it is necessary to know in detail the working conditions. (soil
88 properties, type and amount of waste to be transported, temperature, etc.). It is also
89 necessary to know the properties offered by the different materials available in the market
90 and evaluate their long-term economic viability. Another way forward in the design of
91 these plants is the study of current operating plants and their failures.

92 The failure analysis process consists of collecting and analysing the information available
93 to determine the primary cause of failure as says ASTM Standard E 2332-04 (ASTM
94 Standard E 2332-04, 2004) and Failure Mode and Effect Analysis (FMEA) (McDermott,
95 2011), thus being able to apply corrective actions and preventive measures in the design
96 of future plants. The Ishikawa diagram, also named tree and Fishbone diagram, is a
97 powerful tool to define the cause and effect, which provide a list of possible problems

98 cause or required parameters to ensure the success of the effort against end pipe failure
99 are given, for this case (Ishikawa, 1986).

100 Prediction of erosion attrition becomes a very useful tool in designing and selecting the
101 equipment needed to prevent or reduce the occurrence of such failures. There are many
102 numerical and experimental studies where erosion of pipes was investigated and studied,
103 mainly thanks to the economic investments of the oil and gas companies. However, the
104 mechanism that causes erosive attrition is not yet well defined (Parsi et al., 2014). In
105 general, the numerical models used for the prediction of erosive attrition fall into three
106 categories: empirical, mechanistic and based on Computational Fluid Dynamics (CFD)
107 simulation. As mentioned above, the erosion mechanism is complicated and most models
108 for predicting erosive attrition are a combination of the three categories. It is important to
109 note that in many cases, erosive attrition cannot be avoided, but it can be controlled to
110 keep it within limits that are acceptable to the end user (“DNV GL. DNVGL-RP-O501:
111 Managing sand production and erosion,.” 2007).

112 Since the end of the 20th century, CFD has played an important role in the analysis of
113 erosion caused by solid particles, since it reduces the economic cost associated with
114 laboratory or field experiments. Additionally, CFD models allow understanding the
115 complexity of the fluid dynamics associated with the process and the change in design
116 and operating conditions. On the other hand, the complexity of the erosion phenomenon,
117 as well as the number of variables involved, make obtaining a 100% reliable CFD model
118 a challenging task.

119 The study of erosion using CFD models consists of three main steps: flow modelling,
120 particle tracking, and erosion calculation (Figure S1). Regarding flow modelling, in the
121 present study, a RANS (Reynolds-averaged Navier-Stokes) treatment was used in the
122 Euler reference framework with a stationary model of turbulence of the k - ω family. This

123 model of turbulence was selected to efficiently determine the turbulence of the flow both
124 in the regions near the wall and in the regions far from it. Particle tracking was modelled
125 as a discrete phase whose particles are dragged into a Lagrangian frame of reference by
126 solving ordinary differential equations with Newton law of motion in a transient state. A
127 one-way coupling between flow modelling and particle tracking was considered,
128 assuming that flow affects particle behaviour, but not vice versa, to decrease the
129 computational cost of the model. Therefore, the behaviour of the fluid was first calculated
130 using a stationary study, and then the trajectories of the particles were calculated using a
131 transient study.

132 Regarding erosion calculation, different models are available in the literature, which were
133 developed to calculate by means of simulation the erosion caused by the impact of erosive
134 particles. The vast majority of existing models consider sand as an erosive agent and
135 under special boundary conditions. However, the same models can be adapted so that
136 they can be used for other erosive agents by modifying their corresponding properties. It
137 is important to mention that erosion is a complicated phenomenon that is affected by
138 different parameters and that currently there is no model able to accurately predict erosion
139 under different boundary conditions.

140 Four main models were found in the literature that could be used to describe and analyse
141 the erosion process on different surfaces, such as the one developed by Finnie
142 (1972)(Finnie, 1972), Oka and Yoshida (2005) (Oka et al., 2005; Oka and Yoshida, 2005),
143 Ahlert (1994) (Ahlert, 1994) and the one included in Det Norske Veritas (2007) (Det
144 Norske Veritas, 2007).

145 The main objective of the present study is to explain the origin of pipe failure in two
146 different factories of AWCS, as the identification of the failure phenomena and to carry
147 out the study classification of 90 failure cases by primary cause. Moreover, the ultimate

148 goal of this paper is to help prevent common issues related to erosive attrition by
149 performing simulations based on CFD, followed by recommendations to avoid the most
150 common and frequent failures in the future.

151 **2. Methodology**

152 The composition of the waste proceed in the plants under study is diverse. However,
153 notice that the waste is basically composed by all the residues produced in this area:
154 general waste, envelopes, packaging and containers, and paper and cardboard.

155 The waste makes a variable path depending on the point of discharge at which it is
156 introduced into the system. Therefore, the distance is from 150 m to 2,000 m, passing
157 through the different elbows and junctions that define the route.

158 The waste is different depending on the time of year, the place, etc. For these 2 plants,
159 their location is in Spain, but there are differences in the composition of each of the
160 fractions. For example, a historic center, despite collecting the same fractions, has a
161 completely different composition to that of a newly developed area. This does not affect
162 the pneumatic collection, as its operation is completely automatic. Once the fractions have
163 been predefined, the system self-regulates in order to provide sufficient suction capacity
164 for transport. In the event that one is denser than the other, the system will regulate itself.

165 **2.1.Failure analysis**

166 The determination of failure causes was performed by a failure analysis method in
167 concordance with the ASTM E2332-04 (ASTM Standard E 2332-04, 2004). The process
168 includes the collection and analysis of data about the failed component and the
169 surrounding environment of the component/system.

170 The data were extracted from the pipe failure reports from two AWCS factories (Factory
171 A and Factory B), focusing the study in the failure analysis, extracting information in
172 order to extrapolate to other AWCS factories.

173 The procedure used to analyse and classify the 90 pipe failure cases was based on ASTM
174 E2332-04. The process was divided into four steps. First, organization and analysis of the
175 data collected of the failed component was performed. The technical information studied
176 were operating conditions of the pipe, the employed materials, pipe installation and life
177 record, and factory design, among others. This information is needed to determine the
178 surrounding of the failure. Second, identification of the physical-chemical phenomena
179 involved in the pipe failure by studying the information previously collected. Third,
180 determination of the different causes that could produce or aggravate the physical-
181 chemical phenomena previously identified. Moreover, an Ishikawa diagram (Ishikawa,
182 1986) was carried out to match the causes with different parameters, like materials,
183 operation procedure, pipe system assembly and design. Fourth, cause analysis is
184 performed in general terms for the two factories and specifically for each one.

185 **2.2. Case studies**

186 The pipe characteristics, the type of the waste transported, the welding characteristics and
187 the failure prevention methods used in each factory are summarized (Table S1).

188 The pipes from the two AWCS factories were designed according to the expected amount
189 of waste transported. The design was different for each part of the pipe system (straight
190 stretch, elbow or connections). In addition, the pipe material used, and its characteristics
191 were different in each factory. The welding materials used in both factories were EC-
192 4541 and 66*66 and the method used was Metal Active Gas (MAG).

193 The operational conditions in both factories were the same, where the rate of waste
194 transported was 8 – 10 m/s and the air transported was 25 – 28 m/s. Besides, the waste
195 transported in each factory was different, paper, plastics and general waste in the Factory
196 A and organic fraction and general waste in Factory B.

197 Cathodic protection was used in both factories as a failure prevention method and the
198 Factory A, an attrition-resistant material was used in the critical zones (detected zones
199 with a high risk of failures) as elbows and connections.

200 **2.3. Failure phenomenon and causes classification**

201 **2.3.1. Failure phenomena**

202 Two main physicochemical phenomena involved in the pipe failure were identified:
203 corrosion and attrition, together with a synergic phenomenon between them known as
204 tribocorrosion.

205 **Corrosion**

206 The corrosive causes previously determined were divided into two groups, according to
207 the origin of the corrosion process, inside or outside of the pipe.

208 Regarding the cases located inside pipes, the corrosion could be attributed to acid pH due
209 to the presence of organic matter and its accumulation in cavities. The leached pH during
210 the acidification phase of the organic matter drops up to 5 and could be stabilized between
211 6 and 7.5 at the end of the process (Reyes, 2015).

212 On the other hand, the corrosion cases detected outside the pipes, some land
213 characteristics, such as chemical composition, particle size, aeration level, electric
214 resistivity, humidity and pH must be considered. Moreover, environment agents' actions
215 could produce changes in land characteristics. Another important factor is the stagnate
216 bags formation with a concentration of chloride ions (Cl^-). This Cl^- could produce
217 localized corrosion known as pitting. EN 14301 (304) and EN 14306 (304 L) stainless
218 steel are susceptible to this kind of corrosion.

219 **Attrition**

220 Two principles' typologies of attrition were identified: abrasive and impact attrition.
221 These two typologies are complicated to differentiate because both can happen at the

222 same time. In the two studied cases, the attrition grade is related to properties, shape, size
223 and rate of the particles transported and the geometry of the pipe. Nevertheless, a general
224 tendency of the attrition by particle velocity, is established (Brunett, 1996), see Equation
225 1.

$$226 \qquad \qquad \qquad A = k \cdot v^n \qquad \qquad \qquad (1)$$

227 where A is the erosion rate (m^3/kg), attrition, v is the particle impact velocity (m/s), and k
228 and n are constants that depend on the physical characteristics of the materials involved,
229 for most materials n have a value between 2.2 and 2.8 . The pipes are dealing with glass
230 and ceramic particles that can produce attrition due to its high hardness, 489 – 550 HB.

231 The abrasive attrition happens when a high hardener material at a certain velocity is in
232 contact with a lower hardness material. This contact will produce micro-cuts in the
233 surfaces of this second material. In the studied cases, this phenomenon happens and is
234 aggravated in the elbows and the lowest part of the pipe. Since this phenomenon relates
235 to the pipe materials is needed to consider the different materials employed.

236 The pipes of stainless INOX AISI 304 and St. 37.2 with hardness (Hardness Brinell, HB)
237 between 175 – 200 HB and 100 – 140 HB respectively, and the glass hardness is between
238 480 – 550 HB. Since the hardness values are very different, this could produce a high
239 grade of abrasive attrition or rapid abrasive attrition, when the relation between hardness
240 is lower than 1.2 ($H_{\text{glass}}/H_{\text{pipe}} > 1.2$), (Batchelor et al., 2011).

241 Considering that the critical zones in pipes are coated with attrition-resistant treatments,
242 these hardness values are higher than the glass hardness, so no abrasive attrition should
243 happen. The coatings applied are CDP 4666 DP/DXW and EnDOtec DO*361 with
244 hardness between 628-685 HB and 666 HB, respectively.

245 The welding zones are the most critical, and it is important to select the correct material
246 to perform the welding. Different electrodes and welding materials were used at the two

247 factories studied. The 66*66 and EC-4541 were used with a hardness of 210 HB, 95 HB
248 and 628 HB. Hence, the 66*66, AISI INOX 309 were sub sessile to suffer abrasive
249 attrition or rapid abrasive attrition, but the EC-4541 due to its high hardness no abrasive
250 attrition should happen.

251 The impact attrition happens in high angle elbows, protrusion pipe, pipefittings and in
252 reparation zones where the shapes are not perfectly reconstructed.

253 **2.3.2. Causes classification**

254 Seven potentials causes were detected that aggravate and cause the attrition phenomena
255 combined with abrasive and impact like glass content, waste velocity etc. In the case of
256 the corrosion three causes were identified, and one of the tribocorrosion phenomena
257 (Table S2). However, is important to note that there are inherent limitations in the cause
258 classifications, which must be considered while carrying out this study. Some potential
259 causes such as mean waste density, surface texture of waste, shape of waste particles and
260 metal content were not included in this study, due to the wide diversity of waste shape
261 and texture.

262 The corrosion and attrition phenomena could happen by different causes with very similar
263 effects. To differentiate these cases and know the cause-phenomena-effect interrelation,
264 an Ishikawa diagram was built, and it is shown in **¡Error! No se encuentra el origen de
265 la referencia..**

266 In the Ishikawa diagram, four principals' parameters were considered: material,
267 operation, assembly and design. The materials could produce abrasive attrition due to
268 glass and ceramic waste content, electrochemical corrosion by the organic fraction acidity
269 and localized corrosion by the stagnating bag formation rich in chloride ions. Moreover,
270 the installation operation could produce abrasion and impact attrition owing to the high
271 rate of the waste transported especially in the change of direction zones (elbows). For the

272 installation assembly, the welding defects can produce tribocorrosion and the pipe
273 protrusion and pipefitting can produce impact. The installation design could produce
274 abrasive and impact attrition because of change of direction and abrasive attrition to lack
275 of attrition-resistant materials.

276 **2.4.Numerical modelling**

277 In this study, the erosion ratio caused by the impact of particles on the sample surface
278 was predicted using the Oka erosion model (Finnie, 1972; Oka and Yoshida, 2005),
279 assuming the values and materials properties provided in supplementary tables (Tables
280 S3 and S4) for the different model parameters. The reason for using Oka erosion model
281 is the higher number of model variables that are taken into account, which allow more
282 flexibility and accuracy of the numerical analysis.

283 The simulations were performed using COMSOL Multiphysics 5.3 finite element
284 software on a computer with an AMD FX™ Six-Core Processor (3.30 GHz) with 8 GB
285 of installed RAM. For the simulations carried out for the present study, it was considered
286 that the energy equation in the Navier-Stokes equations was not solved and the surface of
287 the pipe was not considered as such, since the software used to carry out the simulations
288 considers the wall as the last layer of the fluid. Therefore, no pipe thickness was specified.
289 Also, it was assumed that the fluid was incompressible, had a constant temperature of 20
290 °C and the fluid velocity was 25 m/s, while that of the particles is adjusted according to
291 the fluid velocity profiles. In the walls of the different components, the non-slip condition
292 was established from the point of view of the fluid and the rebound condition from the
293 particles.

294 Under the impossibility to simulate real-size waste particles, which may be as big as
295 tens of centimetres, much smaller particles (below 1 cm) with physical properties that
296 could emulate the behaviour of soft and hard material available in the waste were

297 considered in the simulations. Therefore, a comparative study of the erosion produced by
298 particles with different properties (for instance different hardness values) was performed,
299 considering materials with very different hardness values such as glass and plastic.

300 The glass particles were assumed as rectangular prisms with dimensions 5 mm × 7
301 mm × 3 mm, with a mass of 0.26 gr, and with a moment of inertia of 1.76×10^{-9} kg·m²,
302 while plastic particles were assumed as spheres of 5.85 mm diameter. Particles were
303 tracked for 0.4 s for computational efficiency issues. Also, it was assumed at any pipe
304 inlet, the particles are located at the lower part of the pipe cross-section and occupy a
305 surface corresponding to 25% of the pipe cross-section, with a production rate of 0.01
306 kg/s. The component walls were assumed completely smooth with no welding at the joints
307 between components.

308 Three geometries were considered for the different simulations, which are the most
309 relevant components of the system considered in the case studies: elbows of different
310 angles (15°, 30°, 45°, 60°, and 90°), a 30° connection, and a straight stretch with a change
311 in the direction of 5° with respect to the horizontal plane. All these elements were assumed
312 to be preceded, and followed by a straight pipe section to study the erosive effects of fluid
313 and particles in the sections before and after them. A schematic of the geometries that
314 were studied, as well as the relevant geometric parameters are provided in supplementary
315 Figure S2.

316 Physically controlled mesh with an extra fine cell size was used for simulations of the 90°
317 elbow, the connection, and the straight stretch. For the rest of elbow angles (15°, 30°, 45°,
318 and 60°), a coarse mesh was used, since in those cases a more qualitative study on erosion
319 was intended.

320 **3. Results and discussion**

321 **3.1. Failure analysis**

322 The 90 cases studied were classified by failure cause, see Figure 2. The 93% of the failures
323 analysed are due to attrition phenomenon where the predominant cause is the attrition in
324 elbows. This excessive attrition located in these zones is due to the glass content, waste
325 rate and in small angles in the elbows, due to the impact of high hardness waste to the
326 pipe walls. On the other hand, the corrosion and tribocorrosion correspond to less than
327 10% of the cases studied. The failures due to the assembly or design could be easily
328 avoided in future AVC factories taking the corresponding measures as well as the faulty
329 welding, pipe protrusion and pipefitting.

330 The failure cases were also classified by the components, to know the weakest parts of
331 the factories. The 85% of the failure cases are concentrated in three components: elbows
332 (37%), straight stretches (33%) and connections (15%). The main failure cause in straight
333 stretches is pipefitting, while in elbows and connections the only failure cause is the high
334 attrition (Figure S3). Additionally, the major part of the failures cases in pipe joins are
335 due to defective welding and, as expected, the localized corrosion and pipe protrusion are
336 located in straight stretches, because of their high probability to suffer these causes due
337 to their high extension compared to other components.

338 As mentioned before, the major failed component is the elbow. For this reason, a deeper
339 study was needed to know the most affected typology of the elbow. Elbows with a 30°
340 angle are the most affected ones, followed by the 90° elbow and the connections (Figure
341 S4).

342 Figure 3 presents the percentage of failure cause for all the failure cases studied in
343 Factory A and B. Only 29 of the analysed cases were produced in factory A. The 29
344 failures occurred during 10 years. During the three first years there were any failure, and

345 after that there were between 6-7 failure per year maximum. In factory B were analysed
346 61 cases. The 96% and 92 % of the cases were due to attrition that collect failures by pipe
347 protrusion, pipefitting, lack of attrition-resistant material and abrasive attrition,
348 respectively. In factory A the most common causes of attrition were pipefitting (48%)
349 and change of direction (41%). The lack of attrition-resistant materials corresponds to 7%
350 of the cases and only 4% of cases correspond to localized corrosion due to non-correct
351 welding. In factory B the attrition cases are mainly due to direction changes (66%) and
352 due to assembly errors (33%), like pipefitting and pipe protrusion. 5% of cases failed
353 were caused by tribocorrosion in faulty welding, and only 3% of failures are due to
354 localized corrosion.

355 **B**

356 **3.2.Numerical simulations**

357 Figure 4 shows the results of the simulations performed for the 90° elbow assuming
358 particles made of glass. There are two main zones significantly affected by erosion: zone
359 A and zone B. Zone A comprises the part of the elbow between angles from 25° to 55°.
360 Zone B comprises the part of the elbow starting from 75° to 90°, the upper part of the first
361 150 cm of the straight pipe section after the elbow, and the lower part of the same straight
362 section after the first 150 cm. It is evident that the most affected area is zone A, with
363 erosion rate values up to 18 times higher than in zone B. Within zone A itself, the most
364 affected area is the upper half, with values 1.5 to 18 times higher than the bottom half.
365 The explanation is that in the initial part of the elbow (0° - 25°) the erosion takes place by
366 friction since particles move mainly parallel to the surface. As the curvature of the elbow
367 increases, the particles no longer produce erosion by friction, but also by direct impact
368 (collision). Around 45°, there is a limit for a direct collision of particles with the pipe

369 surface, after which particles interact with the elbow surface due to secondary collisions
370 and friction.

371 Figure 5 shows the erosion rate distribution according to the results of the simulations
372 performed for the 30° connection, in the case when glass particles enter from the lateral
373 branch and air flows through the main pipe. In this case, the region where particles coming
374 from the secondary branch collide with the surface of the main pipe is where erosion has
375 a greater impact. The most affected area is comprised between 62% and 82% of the total
376 length of the element (L1 in Figure S2), covering almost the entire lower half of the
377 surface of the main pipe. In the case in which the erosive particles enter from the straight
378 section of the 30° connection (not shown here), practically no erosion was observed due
379 to the fact that there are no critical points where particles collide with the pipe surface.

380 Figure 6 shows the erosion rate distribution according to the results of the simulations
381 performed for the straight stretch with a change in the direction of 5° for glass particles.
382 The change of direction of particle movement mostly affect the lower part of the pipe area
383 where the change takes place, as well as the lower part of the straight pipe section that
384 follows. Specifically, the most affected area is at the junction between the two straight
385 pipe sections, and in the first 30% of the total length of the straight pipe section that
386 follows. However, it is important to highlight that the effect caused by the change in the
387 direction is substantially less than in the previous component, showing the influence of
388 geometry on the rate of erosion.

389 To study the erosive effect of the type of waste that flows inside the pipes, a simulation
390 was performed for the 90° elbow considering that particles were made of plastic and was
391 compared with the erosion rate obtained using glass (Figure S5). The erosion rate
392 produced by glass particles is much higher than the one produced by plastic particles,

393 highlighting the need to avoid the presence of glass in the waste collection system to
394 prevent damages in the pipes due to erosion.

395 The effect of using a different pipe material of higher hardness value was also
396 investigated. The results of the simulation performed for the 90° elbow made of a material
397 with a hardness value three times higher than the base-case material (St. 37.2 steel) is
398 shown in Figure 7. The comparison with the base case indicates that increasing the pipe
399 material hardness by a factor of 3, the maximum erosion peaks are reduced by almost
400 50%.

401 Lastly, the effect of a change in the radius of curvature of a 90° elbow on the erosion rate
402 was also investigated with a simulation for a radius of curvature that is double than the
403 base case, for the same pipe diameter. The erosion rate decreases as the radius of curvature
404 increases, because for higher values of the radius of curvature, the direct impact of solid
405 particles on the pipe surface is reduced (Figure S6). However, a higher radius of curvature
406 also implies an increase in the total pipe length, and therefore an increase in the final
407 economic cost. Therefore, a compromise should be reached between the reduction of
408 erosion rate and the increase of costs produced by an increase of the radius of curvature.

409 **4. Conclusions**

410 The major part (93%) of failure registered was originated due to the abrasive attrition,
411 mainly in elbows and connections (58%) and in pipefitting (31%). This phenomenon
412 happens due to different factors, but there are two factors that are present in all the
413 situations, these are the high glass content in the waste and the high transportation rate 8-
414 10 m/s. If this content is reduced, the failures in the system will be drastically decreased.
415 The presence of glass in the waste is the main cause of attrition, due to its high hardness.
416 To reduce this effect, the glass content in the waste should be reduced, and the materials
417 used in the pipes should have with higher hardness ($1 < H_{\text{glass}}/H_{\text{metal}} < 1,2$) than the hardness

418 of the pipes used in these two factories. This fact is corroborated with the numerical
419 simulation reflects: non-erosion was detected in the case of a 90° elbow with a 0% of
420 glass content in the waste transported.

421 The results reveals that the waste transported rate is a critical parameter in terms of
422 attrition since this parameter is directly related to the attrition grade. The higher the rate
423 of waste transported, the higher the attrition in an exponential way. Therefore, to reduce
424 by 20 – 25% the attrition grade involves a 10% reduction of the transport rate. So, the
425 optimization of this rate will be convenient for each part of the pipe system, or almost in
426 the critical zones, like elbows and connections.

427 At the light of the results here presented, the optimization of the base material used in the
428 pneumatic system as well as the reinforcement with of attrition resistant materials in
429 elbows and connections are the main recommendations to be considered for building new
430 AWCS.

431 **Acknowledgements**

432 The authors at the Universitat de Barcelona would like to thank the Catalan Government
433 for the quality accreditation given to their research group DIOPMA (2017 SGR 0118).
434 DIOPMA is certified agent TECNIO in the category of technology developers from the
435 Government of Catalonia. The authors at the Universitat de Lleida would like to thank
436 the Catalan Government for the quality accreditation given to their research group (2017
437 SGR 1537). GREiA is certified agent TECNIO in the category of technology developers
438 from the Government of Catalonia. This work is partially supported by ICREA under the
439 ICREA Academia programme.

440 **References**

441 Ahlert, K., 1994. Effect of Particle Impingement Angle and Surface Wetting on Solid
442 Particle Erosion of AISI 1018 Steel. The University of Tulsa.

443 ASTM Standard E 2332-04, 2004. Standard Practice for Investigation and Analysis of
444 Physical Component Failures. ASTM Int. 4–5. <https://doi.org/10.1520/E2332-04.2>

445 Batchelor, A.W., Loh, N.L., Chandrasekaran, M., 2011. Materials Degradation and Its
446 Control by Surface Engineering, Materials Degradation and Its Control by Surface
447 Engineering. IMPERIAL COLLEGE PRESS. <https://doi.org/10.1142/p689>

448 Bravo, A.C., 1975. Environmental systems at Walt Disney world.
449 J.ENVIRONM.ENGNG DIV.ASCE 101, 887–895.

450 Brunett, A.J., 1996. The use of laboratory erosion test for the prediction of wear in
451 pneumatic conveyor bend. University of Greenwich.

452 Chàfer, M., Sole-Mauri, F., Solé, A., Boer, D., Cabeza, L.F., 2019. Life cycle
453 assessment (LCA)of a pneumatic municipal waste collection system compared to
454 traditional truck collection. Sensitivity study of the influence of the energy source.
455 J. Clean. Prod. 231, 1122–1135. <https://doi.org/10.1016/j.jclepro.2019.05.304>

456 Dallaire, G., 1974. Pneumatic waste collection on the rise. Civ. Eng. 44, 82–85.

457 Det Norske Veritas, 2007. Recommended Practice RP O501 Erosive Wear in Piping
458 Systems Technical report, DNV RP O501–Revision 4.2.

459 DNV GL. DNVGL-RP-O501: Managing sand production and erosion. [WWW
460 Document], 2007. URL [http://rules.dnvgl.com/docs/pdf/dnvgl/RP/2015-](http://rules.dnvgl.com/docs/pdf/dnvgl/RP/2015-08/DNVGL-RP-O501.pdf)
461 [08/DNVGL-RP-O501.pdf](http://rules.dnvgl.com/docs/pdf/dnvgl/RP/2015-08/DNVGL-RP-O501.pdf) (accessed 7.11.18).

462 Fernández, C., Manyà, F., Mateu, C., Sole-Mauri, F., 2015. Approximate dynamic
463 programming for automated vacuum waste collection systems .
464 <https://doi.org/10.1016/j.envsoft.2015.01.013>

465 Fernández, C., Manyà, F., Mateu, C., Sole-Mauri, F., 2014. Modeling energy
466 consumption in automated vacuum waste collection systems. Environ. Model.
467 Softw. 56, 63–73. <https://doi.org/10.1016/j.envsoft.2013.11.013>

468 Finnie, I., 1972. Some observations on the erosion of ductile metals. *Wear* 19, 81–90.
469 [https://doi.org/10.1016/0043-1648\(72\)90444-9](https://doi.org/10.1016/0043-1648(72)90444-9)

470 Hedden, R.E., 1975. Feasibility of Pneumatic Transport of Refuse in High-Rise
471 Structures. *AGARD Rep.* 767–781.

472 Iriarte, A., Gabarrell, X., Rieradevall, J., 2009. LCA of selective waste collection
473 systems in dense urban areas. *Waste Manag.* 29, 903–914.
474 <https://doi.org/10.1016/j.wasman.2008.06.002>

475 Ishikawa, K., 1986. Guide to quality control. Asian productivity organization. *Ann*
476 *Arbor.*

477 Jackson, S.B., 2004. An In-Depth Report on the Development, Advancement, and
478 Implementation of Pneumatic Waste Collection Systems and a Proposed Program
479 for the Practical Evaluation of Such a System in Terms of Waste Disposal
480 Parameters, Engineering Design, and Economic Costs. *Indep. Res. Proj.* 246, 350.
481 [https://doi.org/10.1016/S0140-6736\(45\)91671-0](https://doi.org/10.1016/S0140-6736(45)91671-0)

482 Kogler, T., 2007. Waste Collection A Report: with Support from ISWA Working Group
483 on Collection and Transportation Technology. *ISWA Rep.*

484 Kown, B. T; Kass, E.A., 1973. Put Refuse In a Pipe, Let Air do the Work. *Am. City* 88,
485 86–87.

486 Laux-bachand, R., 2003. How Does the AVAC System Work, Anyway? *Main Str.*
487 *WIRE* 23, 1–4.

488 McDermott, R., 2011. The basics of FMEA, CRC Press.
489 <https://doi.org/10.1017/CBO9781107415324.004>

490 Nakou, D., Benardos, A., Kaliampakos, D., 2014. Assessing the financial and
491 environmental performance of underground automated vacuum waste collection
492 systems. *Tunn. Undergr. Sp. Technol.* 41, 263–271.

493 <https://doi.org/10.1016/j.tust.2013.12.005>

494 Njobuenwu, D.O., Fairweather, M., 2012. Modelling of pipe bend erosion by dilute
495 particle suspensions. *Comput. Chem. Eng.* 42, 235–247.
496 <https://doi.org/10.1016/j.compchemeng.2012.02.006>

497 Oh, J.H., Lee, E.J., Oh, J.I., Kim, J.O., Jang, A., 2016. A comparative study on per
498 capita waste generation according to a waste collecting system in Korea. *Environ.*
499 *Sci. Pollut. Res.* 23, 7074–7080. <https://doi.org/10.1007/s11356-015-4834-7>

500 Oka, Y.I., Okamura, K., Yoshida, T., 2005. Practical estimation of erosion damage
501 caused by solid particle impact: Part 1: Effects of impact parameters on a
502 predictive equation, in: *Wear*. Elsevier, pp. 95–101.
503 <https://doi.org/10.1016/j.wear.2005.01.039>

504 Oka, Y.I., Yoshida, T., 2005. Practical estimation of erosion damage caused by solid
505 particle impact: Part 2: Mechanical properties of materials directly associated with
506 erosion damage, in: *Wear*. Elsevier, pp. 102–109.
507 <https://doi.org/10.1016/j.wear.2005.01.040>

508 Parsi, M., Najmi, K., Najafifard, F., Hassani, S., McLaury, B.S., Shirazi, S.A., 2014. A
509 comprehensive review of solid particle erosion modeling for oil and gas wells and
510 pipelines applications. *J. Nat. Gas Sci. Eng.*
511 <https://doi.org/10.1016/j.jngse.2014.10.001>

512 Popa, C.L., Carutasu, G., Cotet, C.E., Carutasu, N.L., Dobrescu, T., 2017. Smart city
513 platform development for an automated waste collection system. *Sustain.* 9, 1–15.
514 <https://doi.org/10.3390/su9112064>

515 Punkkinen, H., Merta, E., Teerioja, N., Moliis, K., Kuvaja, E., 2012. Environmental
516 sustainability comparison of a hypothetical pneumatic waste collection system and
517 a door-to-door system. *Waste Manag.* 32, 1775–1781.

518 <https://doi.org/10.1016/j.wasman.2012.05.003>

519 Reyes, M., 2015. Lixiviados en plantas de residuos. Una contribución para la selección
520 del proceso de tratamiento. Universitat Politècnica de València.

521 Teerioja, N., Moliis, K., Kuvaja, E., Ollikainen, M., Punkkinen, H., Merta, E., 2012.
522 Pneumatic vs. door-to-door waste collection systems in existing urban areas: A
523 comparison of economic performance. *Waste Manag.* 32, 1782–1791.
524 <https://doi.org/10.1016/j.wasman.2012.05.027>

525 Zandi, I., Hayden, J.A., 1969. Are pipelines the answer to waste? *Environ. Sci. Technol.*
526 3, 812–819. <https://doi.org/10.1021/es60032a604>

527 Zdravecká, E., Slota, J., Tkáčová, J., 2014. Erosive failure of steel pipeline by solid
528 pulverized particles. *Eng. Fail. Anal.* 46, 18–25.
529 <https://doi.org/10.1016/j.engfailanal.2014.07.016>

530

CAUSE

EFFECT

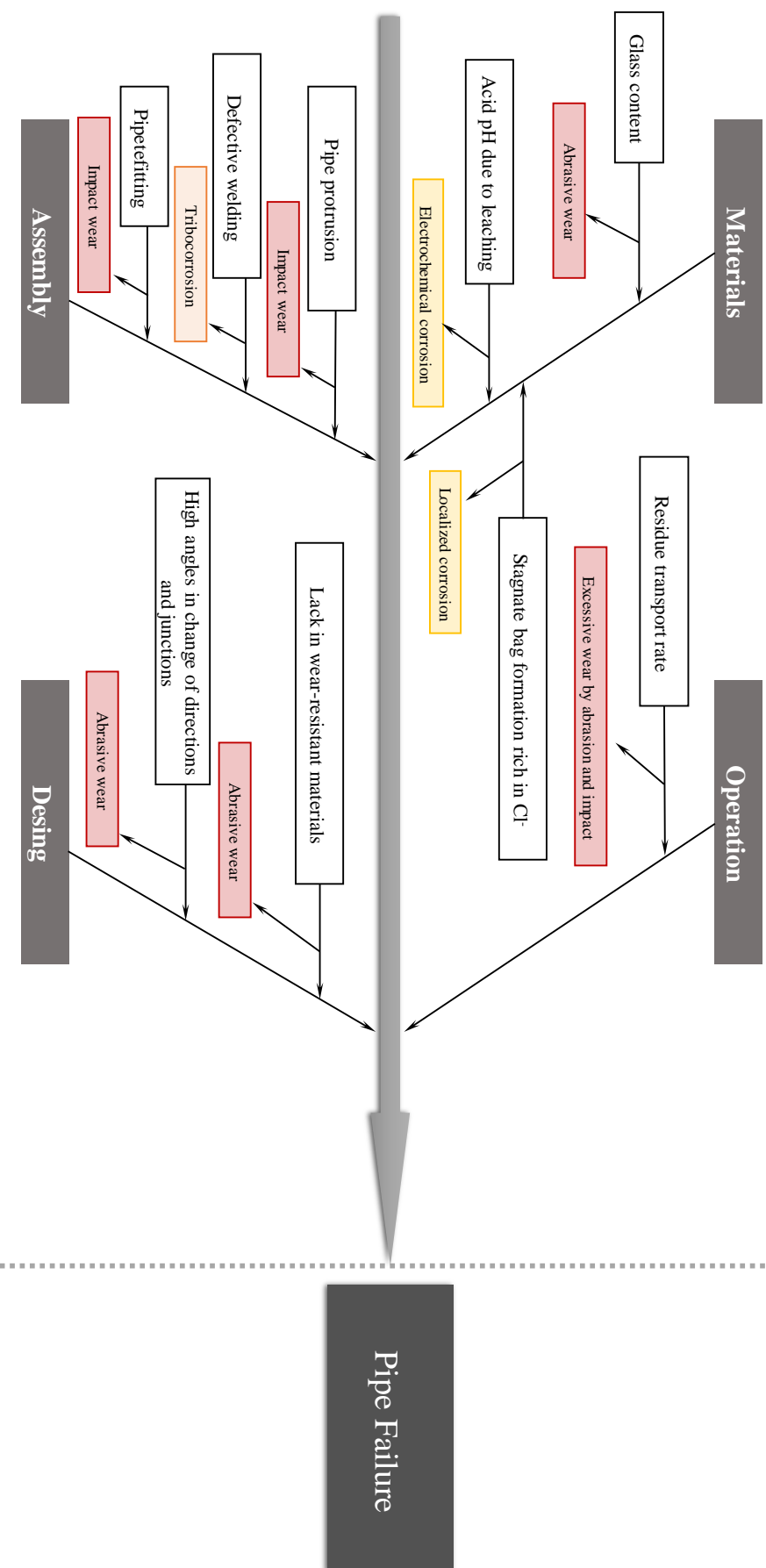
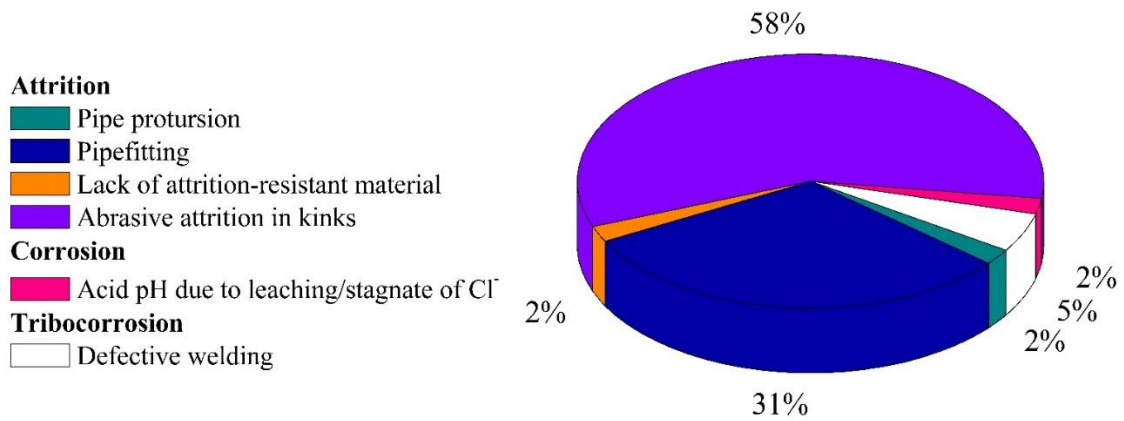
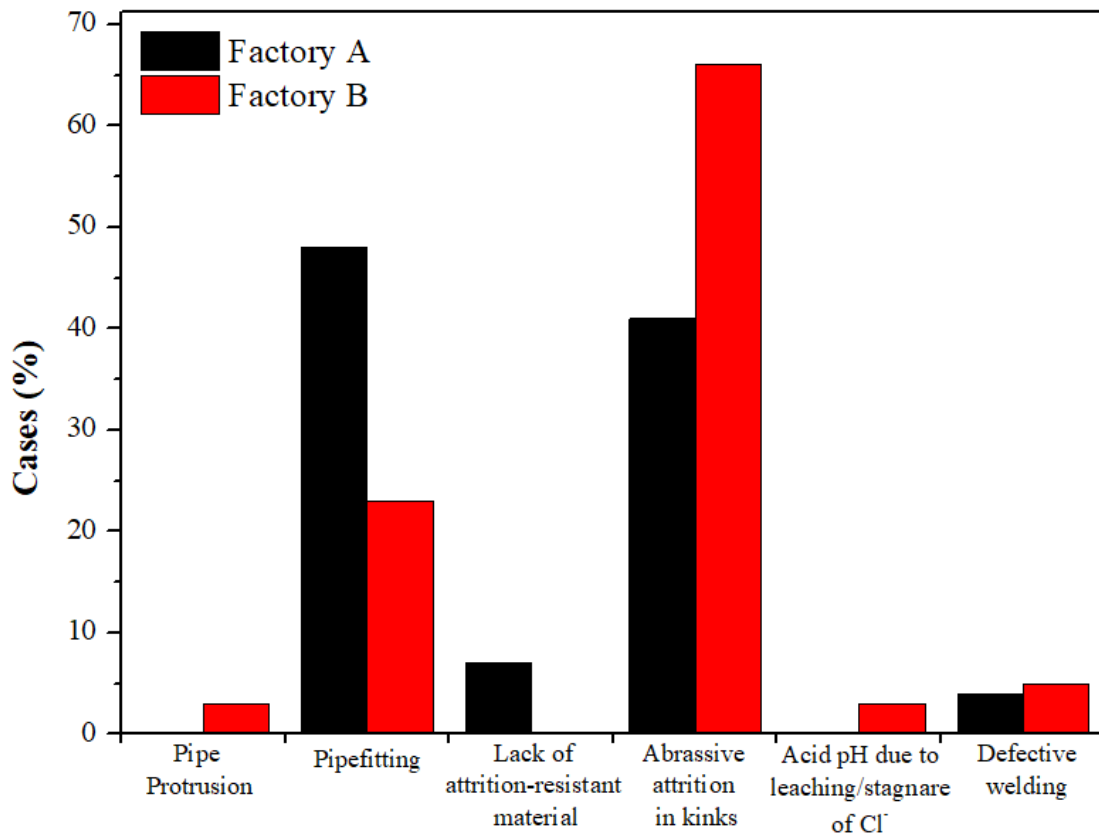


Figure 1. Ishikawa diagram of potential causes and effects of pipes in AWWCS systems



532

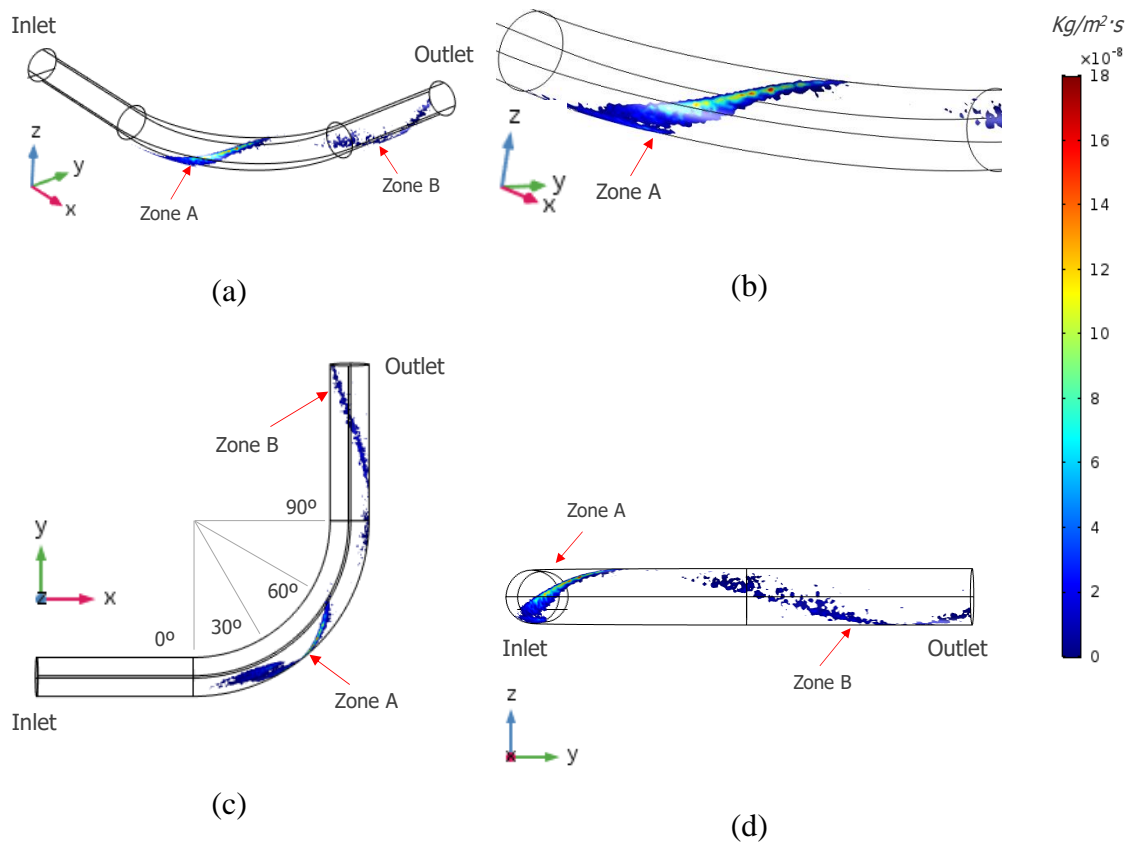
533 **Figure 2. Classification of the 90 cases studied in both factories**



534

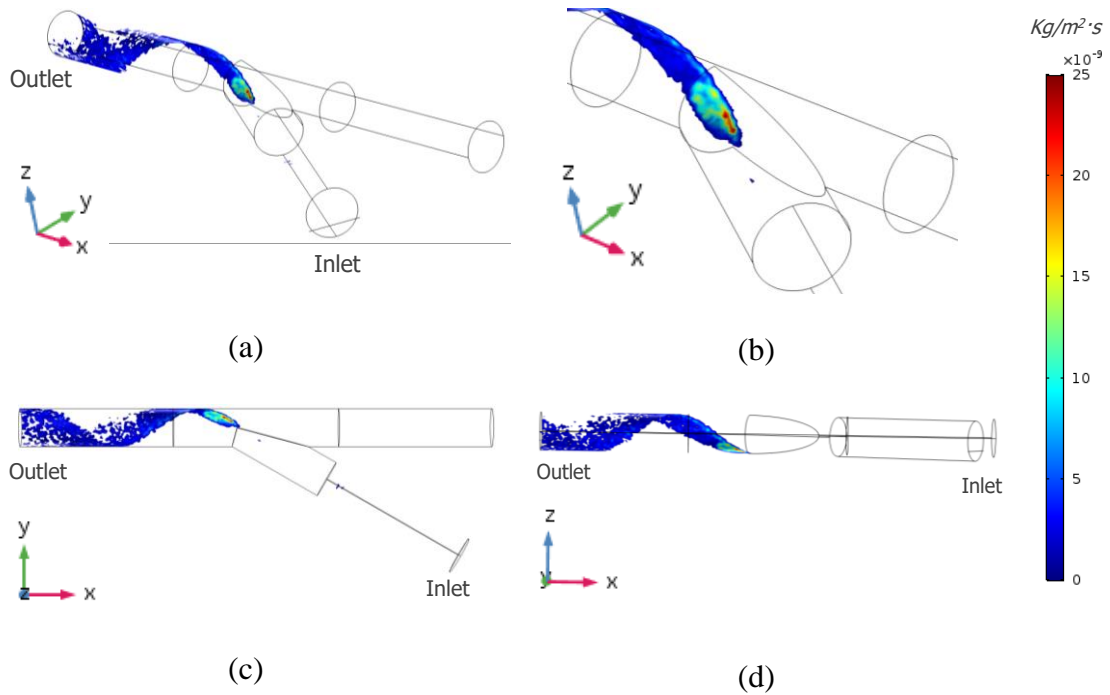
535 **Figure 3. Classification of the 29 cases in the Factory A and 61 cases in Factory**

536



537 **Figure 4. Erosion rate on the 90° elbow surface and on the preceding and**
 538 **subsequent straight sections. (a) Three-dimensional view; (b) amplified three-**
 539 **dimensional view of the area most affected by erosion; (c) top view; and (d) side**
 540 **view. Note: all values less than $1 \cdot 10^{-8} \text{ kg}/(\text{m} \cdot \text{s})$ have been removed for better**
 541 **visualization.**

542
 543
 544
 545
 546



547 **Figure 5. Erosion rate on the surface of the 30° connection and on the preceding**
 548 **and subsequent straight sections for particles entering from the lateral branch. (a)**
 549 **Three-dimensional view; (b) enlarged three-dimensional view of the area most**
 550 **affected by erosion; (c) top view; and (d) side view. Note: the measurement scale is**
 551 **different from that of the 90° elbow for better visualization.**

552

553

554

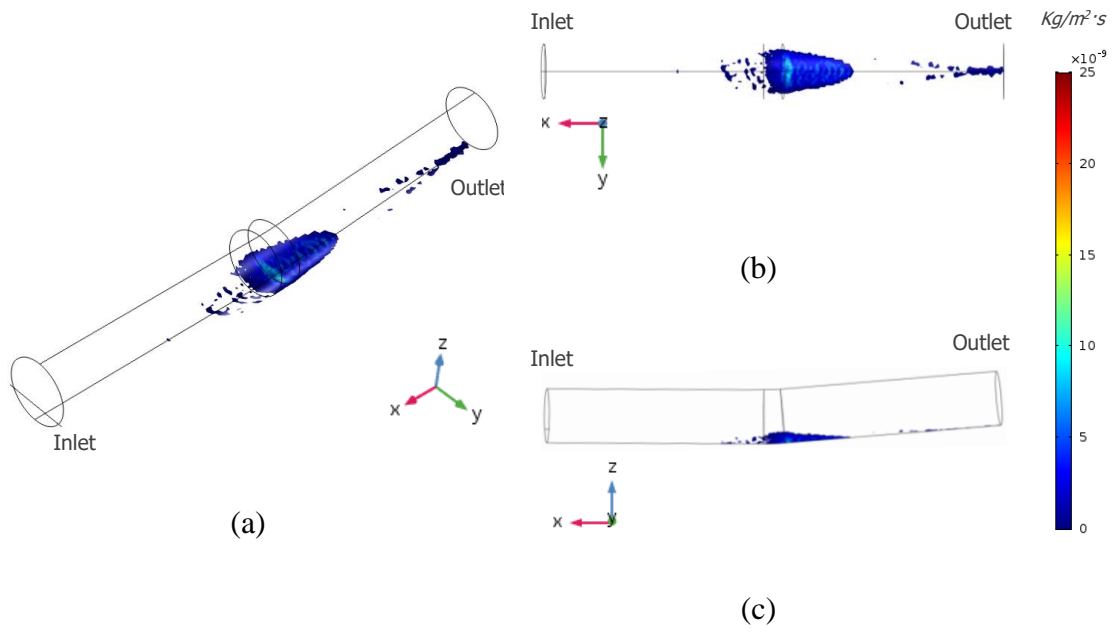
555

556

557

558

559



560 **Figure 6. Erosion rate on the surface of the preceding and subsequent straight**
 561 **sections of a 5° change in direction. (a) Three-dimensional view; (b) top view; and**
 562 **(c) side view.**

563

564

565

566

567

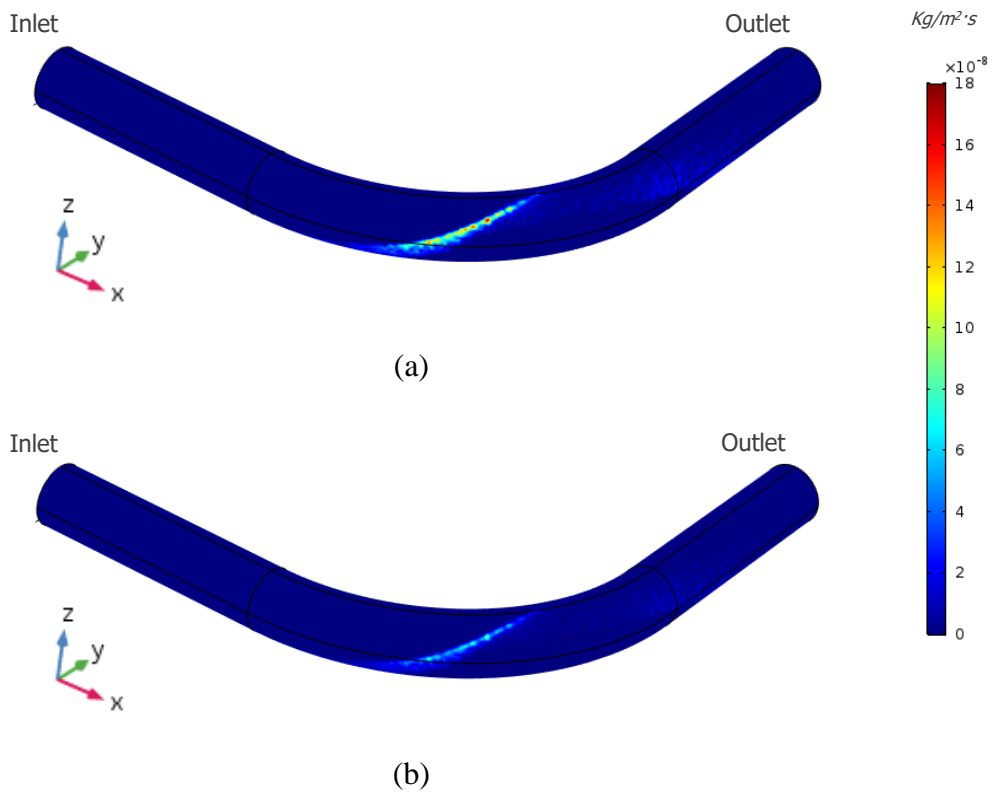
568

569

570

571

572



573 **Figure 7. Erosion rate on the 90° elbow surface and on the preceding and**
 574 **subsequent straight sections for a pipe made of (a) steel St. 37.2 and (b) a material**
 575 **with a hardness three times higher than steel St. 37.2.**

576